Monte Carlo simulation and analysis of free-form surface registration

D Brujic and **M Ristic**
Mechanical Engineering Department, Imperial College of Science, Technology and Medicine, London

Abstract: Accurate dimensional inspection and error analysis of free-form surfaces requires accurate registration of the component in hand. Registration of surfaces defined as non-uniform rational B-splines (NURBS) has been realized through an implementation of the iterative closest point method (ICP). The paper presents performance analysis of the ICP registration method using Monte Carlo simulation. A large number of simulations were performed on an example of a precision engineering component, an aero-engine turbine blade, which was judged to possess a useful combination of geometric characteristics such that the results of the analysis had generic significance. Data sets were obtained through CAD (computer aided design)-based inspection. Confidence intervals for estimated transformation parameters, maximum error between a measured point and the nominal surface (which is extremely important for inspection) mean error and several other performance criteria are presented. The influence of shape, number of measured points, measurement noise and some less obvious, but not less important, factors affecting confidence intervals are identified through statistical analysis.

Keywords: registration, inspection, Monte Carlo simulation, free-form surfaces, NURBS

NOTATION

F	cost function
N	number of points
P_i	ith measurement point
q_i	ith corresponding point on the model
$\mathbf{R}$	the rotation matrix
s^2	unbiased sample variance
$t_{\alpha/2}$	Student t-statistic value
$\boldsymbol{T}$	the translation vector
u, v	parametric surface parameters
x, y, z	Cartesian coordinates, translation parameters
$\bar{x}$	sample mean value
α, β, γ	rotation angles
σ	standard deviation

1 INTRODUCTION

Accurate registration of free-form surfaces is an important requirement in many branches of the manufacturing industry. The requirement arises at several stages in the product life cycle such as inspection during product and manufacturing process development, inspection in production, and also in the repair of broken or worn out parts. A common feature of these components is the absence of clearly defined reference points. The prime examples are components produced using forming processes (casting, forging, pressing), such as aero-engine compressor and turbine blades, car body panels and others.

Inspection of free-form surfaces requires measurement of a large number of points such that the actual surface may be characterized in full (**1**). This may be performed using one of a number of available contact or non-contact measurement sensors (**2**). In such situations the adoption of CAD (computer aided design)-oriented inspection is widely seen as the appropriate inspection methodology (**3**, **4**). In the cases when the free-form component possesses no clear reference features, the CAD-oriented inspection is based on software best-fitting between the CAD model and the measured points as the required registration technique.

The principal method for best-fitting which is analysed in this paper is least squares (LS) fitting, which was implemented as the iterative closest point (ICP) method (**3**, **4**). LS fitting is well recognized and has received considerable attention in the literature, but relatively little has been published in terms of its performance analysis. The published work tends to be limited to the situation where point correspondences are *a priori* known (**6**–**8**), which is not true in the case of the ICP method. The work by Stoddart *et al*. (**9**) proposes a method to predict the quality of registration but it is primarily concerned with indicating the cases of near degeneracy. A large number of factors (such as

The MS was received on 10 May 1996 and was accepted for publication on 19 August 1997.

measurement noise, number of measured points, object geometry, etc.) can be identified to affect different aspects of ICP registration performance (such as accuracy, convergence rate, etc.), but the effects are not necessarily apparent and straightforward. The influence of the measurement noise, which is in reality always present, is considered to be particularly important for inspection, but this too has received little consideration in the published literature.

Fully analytical evaluation of the performance is extremely difficult, if not impossible, owing to the complexity of the problem. Under these circumstances, Monte Carlo simulation (**10**) was undertaken as an alternative to an analytical evaluation of the LS fitting performance. This is a method of statistical trials, based on the principle of simulating a statistical experiment by computational techniques, and recording the numerical characteristics obtained from this experiment. The solution of numerical problems by this method is closer to physical experiments than to classical computational methods.

Before proceeding with the full presentation of this study, Section 2 summarizes the principle of the best-fitting methods used in this work. The implementation involved a number of important improvements in the computational speed which were mainly realized in relation to the manipulation of model geometry. These improvements are explained in Section 3, in order to clarify the implementation of the algorithms. The conduct of the Monte Carlo simulation is explained in Section 4. The subsequent sections deal with various aspects of the algorithm performance analysis. Section 10 summarizes the most important generic conclusions drawn from this work.

2 METHODS FOR FREE-FORM SURFACE REGISTRATION

During inspection, it is assumed that a sufficiently large number of properly distributed measurements are available. Further, it is assumed that the component is defined as a non-uniform rational B-spline (NURBS) surface and is made available by the original computer aided design (CAD) system as an initial graphics exchange standard (IGES) file. Two registration methods are considered to be of special interest. They are the moment of inertia (MoI) method (**11**) and the LS fitting (**12**).

The principle method of calculating the required transformation is LS fitting. This was realized through the iterative closest point (ICP) method, which has been proved (**4**) always to converge to a local minimum. However, as the global convergence of ICP is not guaranteed, the MoI method is in general available as an alternative first alignment step.

2.1 Moment of inertia method

The MoI method does not rely on the correspondence between the measured and the nominal points. It calculates the first two moments of the distribution geometry for each data set and determines the translation that aligns their centres of mass, and rotation that aligns their principal axes. The method was found to be effective for most shapes with distinct principal axes and reasonably distributed measurements. Although less accurate than LS fitting, MoI was found to provide good results very quickly, even if the misalignment and the number of measured points are very large.

2.2 Least squares fitting

LS fitting can be defined as follows (**4**):

> Given 3D data in a sensor co-ordinate system, which describes a data shape that may correspond to a model shape, and given a model shape in a model co-ordinate system in a different geometric representation, estimate the optimal rotation and translation that aligns the model shape and the data shape minimising the distance between the shapes and thereby allowing determination of the equivalence of the shape via a mean-square distance metric.

Based on the above definition the cost function to be minimized in LS fitting is the model-part distance, which can be expressed as

$$F = \sum_{i=1}^{N} (q_i - \mathbf{R}_i \cdot p_i - \boldsymbol{T})^2 \qquad (1)$$

where

$\boldsymbol{T} = 3 \times 1$ translation vector

$\mathbf{R} = 3 \times 3$ rotation matrix

$p_i = i$th measurement point

$q_i =$ corresponding point on the model

The fitting procedure involves exclusion of two distinct steps in a loop, namely:

(a) evaluation of the corresponding point set $\{q\}$ on the model and
(b) calculation of the required translation $\boldsymbol{T}$ and rotation $\mathbf{R}$ and their application on the measured data set.

The critical step in the procedure is to establish the points on the model that correspond to the measured points. It has been shown (**4**) that by using the closest points on the model as the corresponding points, it is possible to construct an iterative LS fitting algorithm that would always converge to a local minimum. This is the basis of the ICP algorithm as the principal registration method.

3 IMPLEMENTATION OF THE ICP ALGORITHM

The implemented registration algorithm contains a number of important improvements on the original ICP method, aimed at maximizing its computational efficiency and robustness. The full presentation of its implementation would be too large to be included in this paper and is provided in references (**13**) and (**14**). In this section, therefore, only an overview is presented of the most important implementation aspects as a preamble for the subsequent performance analysis.

The first step in ICP, calculation of the closest point, is the most time consuming and there are considerable computational advantages to be gained by adopting appropriate methods for manipulation of the model geometry. The adopted modelling methodology is described in the next sections.

3.1 Geometric modelling and manipulation

The principal modelling entity in this work was taken to be NURBS. In order to overcome the considerable computational burden of performing modelling operations on NURBS surfaces, it was decided to allow dual representations of the model entities. The adopted structure is a polyhedral surface approximation.

The approximation employs an adaptive sampling technique (**15**), in which the fineness of the subdivision can vary over the parameter space. This greatly reduces the number of triangles needed to accurately describe a surface, compared to the uniform grid where the side effect is that the regions of low curvature are over-sampled. The surface is approximated by a mesh of straight line segments joining each pair of adjacent grid points and triangular polyhedra are obtained by splitting each rectangle into two triangles. The acceptance criteria for each region in adaptive sampling require special attention, owing to the requirement that the triangulation is both accurate to a given tolerance and topologically correct with respect to the nominal geometry. Thus in the implemented algorithm the subdivision termination criteria are based on flatness (**16**), as well as on object thickness (**13**). The thickness e of an object, as defined in reference (**17**), is the real positive number such that any maximal ball included either inside or outside the object has a radius larger than or equal to e. The acceptance criterion based on thickness states that the density of the points on the surface must be greater than $1/(2e)$. The approximation obtained under this condition is homeomorphic.

3.2 Calculation of the closest point

The most time consuming operation in ICP is the calculation of the closest point on the NURBS surface. This problem was overcome by performing the fitting in two phases. In the first phase, measured points are fitted to the wiremesh approximation and when a minimum is achieved in the second phase the fitting is switched to NURBS. The algorithm considers the vertex nearest to the given spatial point and the region which is formed by the facets in the vicinity of that vertex. It examines whether the projection of the given point falls on any of the facets surrounding the vertex and, if not, then the region under consideration is expanded to include the adjoining facets. The process may then be repeated until the true nearest point has been found. Admittedly, this algorithm is not guaranteed to succeed and expansion of the search window can sometimes lead to an exhaustive search. For this reason the algorithm is limited to only two window expansions; if the orthogonal projection does not fall on any of the included facets then it is replaced by the nearest point found on one of the included edges. This solution produced good results and it is justified in this case, because this task is performed at early alignment stages when the nearest point on the polyhedron is only an approximation of the true corresponding point.

Calculation of the true closest point in a NURBS surface involves iterative methods, which in turn require an initial guess. With the dual representation of the model, the vertices of the approximate model provide this initial guess. The method was found to be successful provided that fineness of the approximate model satisfies the above-mentioned thickness criterion.

3.3 Calculation of the transformation matrix

The calculation of a rigid body transformation that minimizes the least squared distance between the point pairs, was solved using singular value decomposition (SVD) as suggested in references (**6**) and (**18**). The main reasons for this are that the SVD method is computationally very efficient and that it can be easily generalized to more than three dimensions.

3.4 Improvements of the ICP algorithm

Following the application of the described procedure, the most time consuming part of the computation was found to be the search for the nearest vertex in the approximation. Three major improvements were introduced in order to increase computational efficiency, namely the adaptive window search, multiscale search and variable approximation, and these are documented in reference (**13**).

Special attention was also given to the ICP termination criteria. The usual termination criterion is that the change in mean square error (MSE) must be smaller than some small pre-specified value, but the difficulty remains how to choose that value. If the condition is not strict enough, then it happens that several points, owing to their random positions, are not fitted as accurately as the others. On the contrary, if the condition is too strict then the number of iterations becomes very large.

It has been observed (**19**) that ICP registration minimizes the systematic component of the error while retaining the random component. This means that the MSE after registration approaches the sample standard deviation of the measurement data set, which in turn (for reasonably large data sets) approaches the standard deviation of the measurement noise, σ. Furthermore, for dimensional inspection purposes it is readily assumed that the measuring instrument is sufficiently well characterized such that the value of σ is known. This argument allowed that both the ICP termination criterion and detection of convergence to a local minimum be based on the known value of σ. In this work the ICP procedure was set to terminate when the change in MSE becomes less than $10^{-2}\sigma$. This value is based on experience and in several thousand conducted experiments it produced good results. Of course, this value is applied only at the final registration stage, while at the first stage, when a subset of measured points and the approximate model are used, a suitably larger value is preferable.

The final improvement was introduced in order to avoid convergence to a local minimum. Following the above argument, local minima are detected as the situations when the MSE value is considerably larger than the known value of σ. In such situations a small local perturbation in position is generated and the subsequent convergence is examined. The conclusion is that the experiments presented in this paper have always resulted in a convergence to the global minimum, but there is still no proper guarantee that a global minimum would be achieved for other misalignments and other object geometries.

4 ICP PERFORMANCE ANALYSIS USING MONTE CARLO SIMULATION

The Monte Carlo simulations were conducted with the aim of investigating ICP performance in terms of several criteria that are considered to be of importance in inspection related applications. These criteria are:

(a) mean square error (MSE),
(b) maximum error (important for inspection),
(c) average error,
(d) confidence in the transformation parameter estimates,
(e) number of iterations required to achieve given accuracy.

The simulations analysed the dependence of these performance measures with respect to the following factors:

(a) number of random measurements on the object,
(b) measurement noise (assumed to be Gaussian with known standard deviation, σ),
(c) initial misalignment (three-dimensional translation and rotation),
(d) fineness of approximation of the NURBS model.

4.1 Random number distributions

In order to perform realistic simulations of the measurement process, special attention was paid to the randomness in the generation of the measurement noise and the initial component misalignment. The measurements were simulated to be randomly distributed over the object surface as the most appropriate situation for a generic registration analysis. This was done by randomly generating in the applicable ranges the u and v parameters of the points on the model. Measurement noise was then simulated as a three-dimensional isotropic Gaussian, by adding Gaussian noise of known σ to the x, y and z coordinates of each point.

The correctness of this noise model in reality would clearly depend on the exact type and characteristics of the measuring equipment used. In conducting this work the authors primarily had in mind the measuring system with which they had the most direct experience, namely a conventional coordinate measuring machine (CMM) equipped with a laser triangulation probe (Matsushita LM200). This system was used to perform measurements on the actual turbine blade in question, and also on a special calibration sphere. Application of the χ test on these data confirmed that the sensor noise and the overall measurement noise are very closely represented as Gaussian. Other experiments were also performed in order to characterize the measuring system and they revealed that the portion of the overall measurement error attributed to the CMM itself is very small (being of the order of a few micrometres) when compared to that due to the laser sensor, which was found to be of the order of several tens of micrometres. Strictly speaking therefore, it may be argued that the measurement noise in this system would be more accurately modelled by a Gaussian distribution in the direction of the probe orientation, together with considerably narrower Gaussian distributions in the directions of the CMM axes. However, considering the fact that the points themselves are randomly distributed over the surface, it was concluded that the three-dimensional isotropic distribution does not produce significantly different results, and that at worst it represents a conservative noise model.

No suitable data were available to indicate that a particular distribution should be chosen in generating the random initial misalignment. Therefore it was decided to adopt a uniform distribution over a specified range in this case. This clearly sets the most difficult range of situations for the ICP algorithm in which its performance is evaluated, but it was considered necessary in order to provide definitive answers about its operation.

4.2 Description and conduct of the Monte Carlo simulation

Data sets were obtained by performing simulation of CAD-based inspection. Because of the large number of data sets required, it was decided to conduct all trials on the basis of a single real object, which was carefully chosen to contain various geometric characteristics that would be representative of different situations. The object used was an aero-engine turbine blade airfoil (Fig. 1) with approximate dimensions of $100\,\text{mm} \times 100\,\text{mm} \times 40\,\text{mm}$. The reasons for its selection are summarized as follows:

(a) high precision engineering component,
(b) CAD model defined as NURBS,

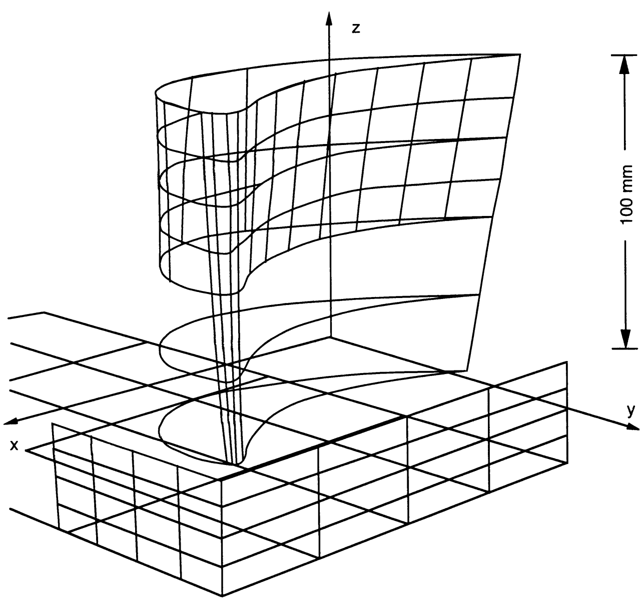

Fig. 1 Turbine blade model used in the Monte Carlo simulations

(c) poor geometric determinacy along the stacking axis (*z*-axis),
(d) contains fine geometric features (small, 0.4 mm, radius of curvature at the trailing edge).

The simulations were conducted through a number of experiments. Each experiment involved 100 simulations by executing the following loop:

1. Compute *N* random points on the surface.
2. Add Gaussian noise with known statistic σ to each point.
3. Apply random rotation about lines parallel to the coordinates axes and passing through the object centre of mass.
4. Apply random translation along all axes.
5. Perform registration.
6. Subtract estimated transformation parameters from the (known) true values and record result, together with MSE, maximum error and number of steps.

After completing the set of simulations in each experiment, the following values were computed:

(a) transformation parameter confidence intervals,
(b) mean error of parameter values estimation,
(c) maximum value of MSE,
(d) mean value of the number of steps.

Several tens of thousands of simulations were conducted and the results are summarized in the following sections. Except where stated otherwise, all simulations involved random initial misalignments w.r.t. each axis in the range ± 3.0 mm translation and $\pm 3.0°$ rotation, while the model was approximated with 5200 vertices corresponding to a tolerance of 0.1 mm and thickness of 0.4 mm.

5 CONVERGENCE ANALYSIS OF THE ICP METHOD

The graphs in Fig. 2 show typical progress of the ICP registration in terms of MSE reduction against the number of iterations. The two curves correspond to different measurement noise values $\sigma = 8\ \mu m$ and $\sigma = 60\ \mu m$. The points A1 and B1 correspond to the switch from fitting to an approximate model to fitting to a NURBS model, while the points A2 and B2 correspond to local minima.

Convergence of the ICP method was evaluated by comparing the MSE and maximum error before the introduction of initial misalignment and after the completion of the fitting iterations. This was repeated for different simulations and the results are shown in Figs 3 and 4. For clarity, only a small number of simulation results are shown here, involving 5000 measured points and noise of $\sigma = 8\ \mu m$. Similar results were obtained for other noise values and numbers of measured points. Our conclusion is that the implemented algorithm resulted in global convergence in all cases.

Figure 3 shows that in each case the value of MSE after fitting closely matches the MSE value before initial misalignment was introduced. In other words, since the initial MSE is given by the standard deviation of the measurement noise, the MSE value after fitting approaches the standard deviation of the measurement noise. This supports the claim that the implemented ICP method achieves global convergence.

Furthermore, the closeness of the graphs in Fig. 4 indicates that the worst measured point (due to a given measurement noise characteristic) results in the maximum error after ICP fitting, i.e. it remains the worst point. This is extremely important in inspection, where the accuracy of each measured point is often an important consideration, and it has been achieved by the strict iteration termination criteria.

An interesting effect is presented in Fig. 5, showing that maximum error increases with the number of measured points. In fact, this is to be expected, because the larger the number of noisy measurements, the greater the probability that some points will be measured with large error.

6 EFFECT OF APPROXIMATION

As explained previously, significant improvements in the overall computational efficiency may be achieved by using an approximate polyhedral model of the object in the first stage of ICP. However, as the search for the nearest vertex became the time critical task in this case, it was important to assess the dependence of the fitting accuracy on the fineness of approximation. In order to study these effects, the NURBS model was approximated by polygonal meshes comprising different numbers of vertices. For each case, 1200 simulations with random initial misalignments and

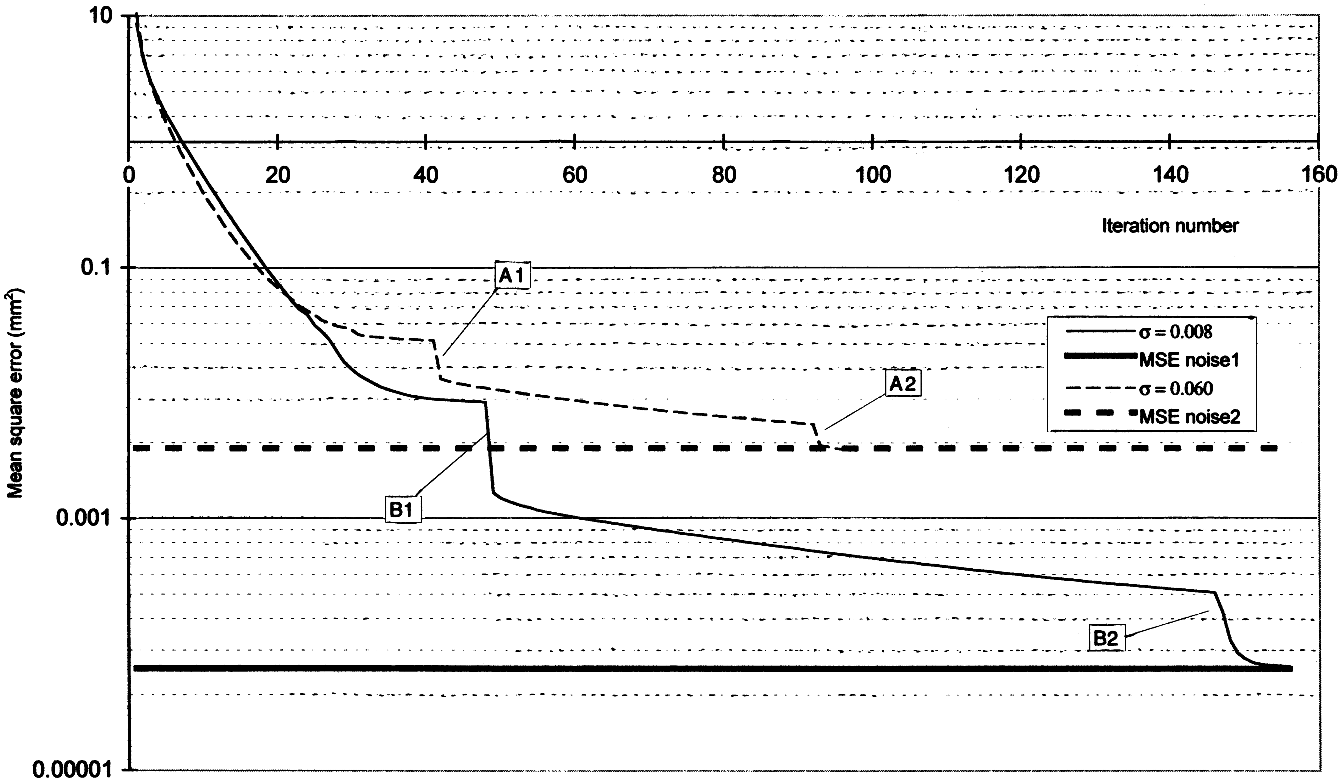

Fig. 2 Typical reduction of MSE versus iteration step number for different noise values

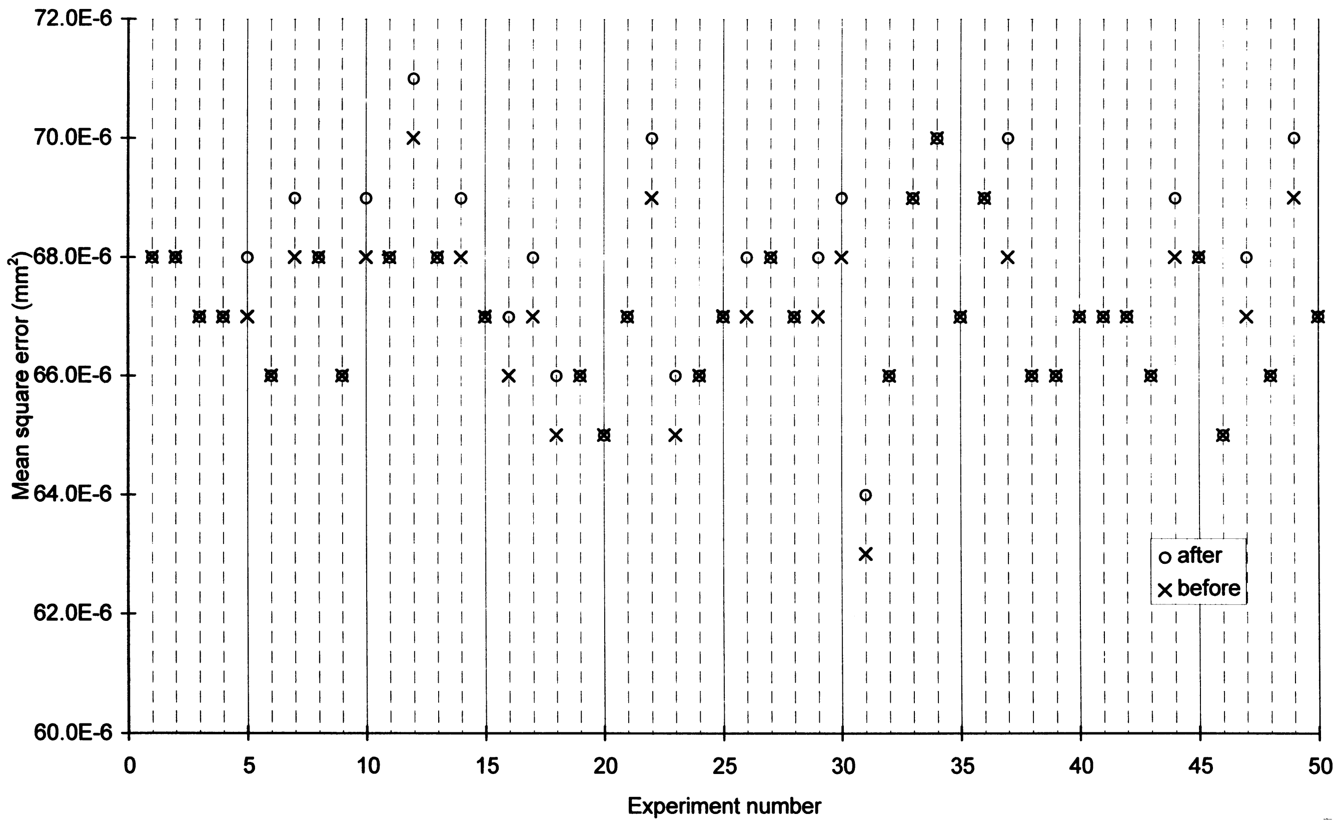

Fig. 3 MSE before misalignment and after ICP fitting in 50 simulations

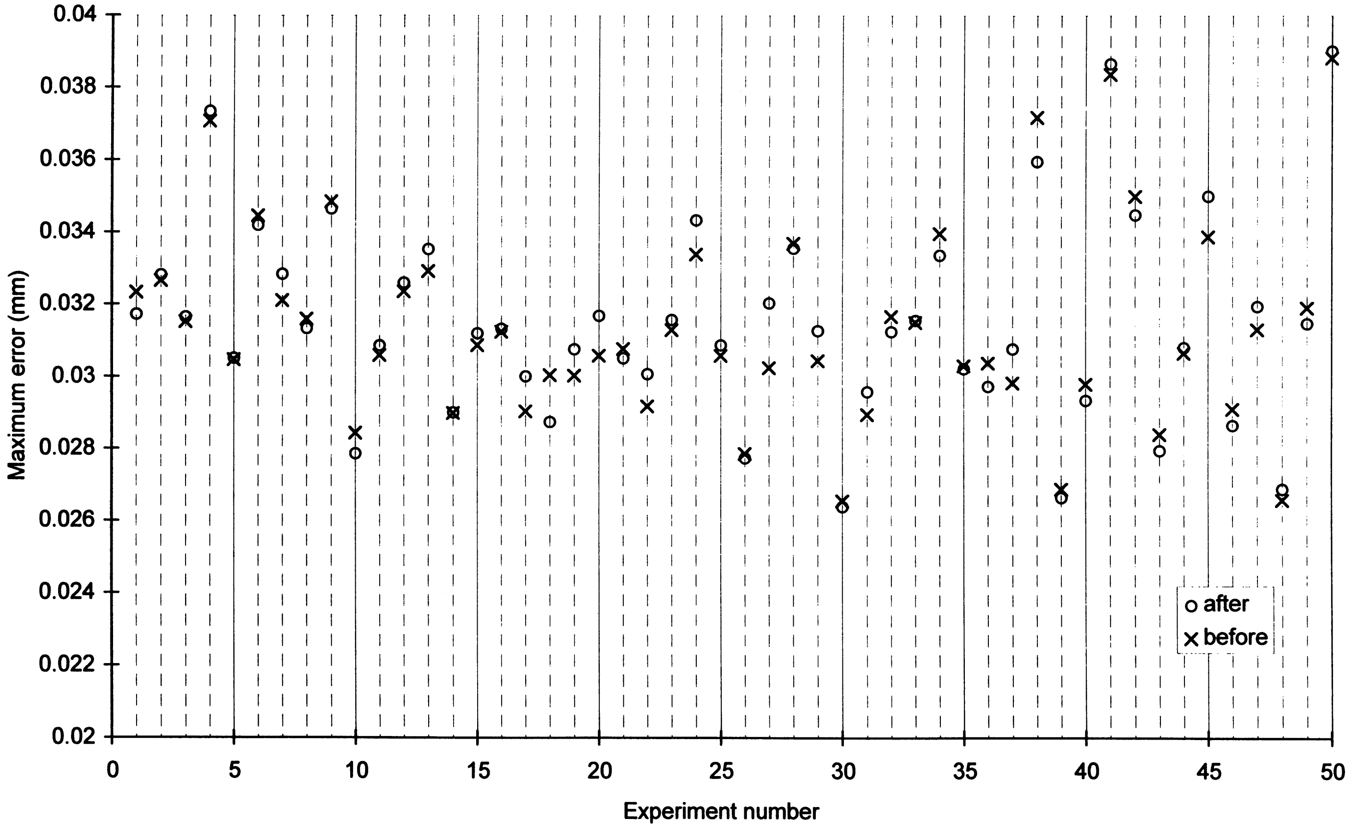

Fig. 4 Maximum error before misalignment and after ICP fitting in 50 simulations

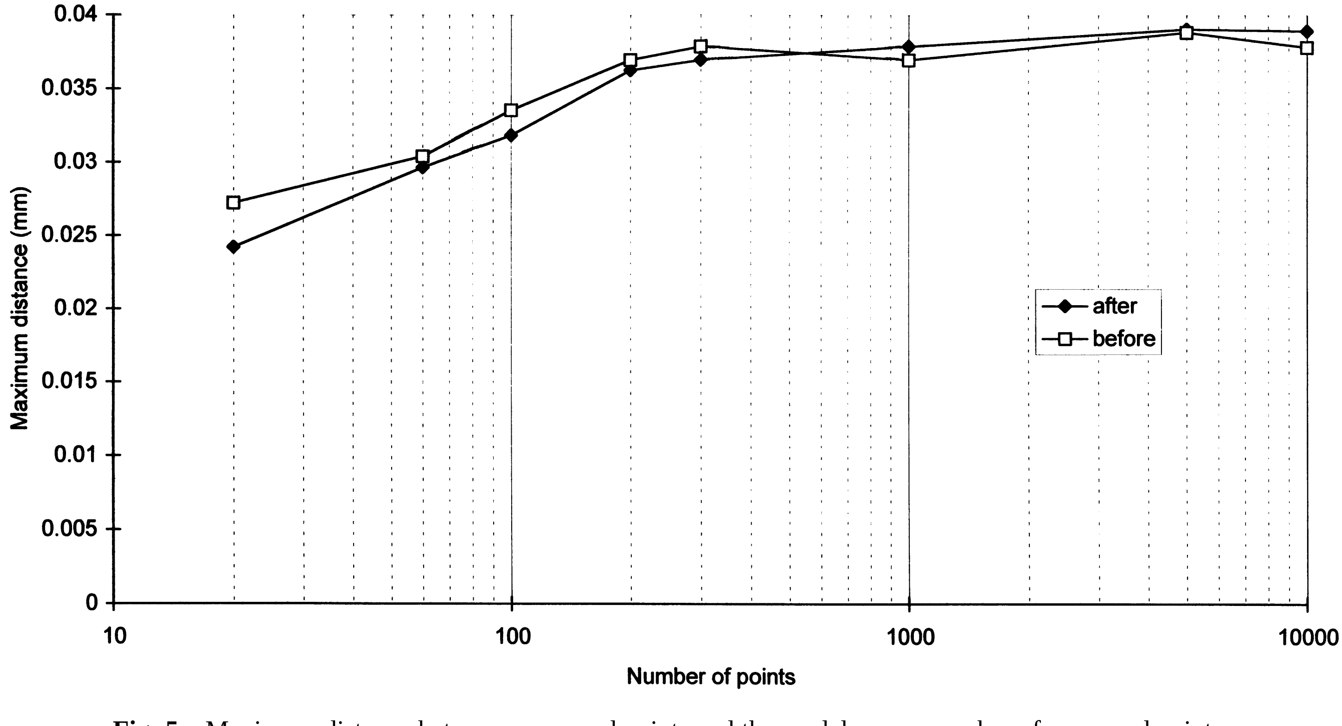

Fig. 5 Maximum distance between measured points and the model versus number of measured points, before initial misalignment and after fitting (noise $\sigma = 8\ \mu m$)

measurement noise of $\sigma = 8\,\mu$m were performed and ICP fitting was applied. The overall results are shown in Fig. 6 in terms of the largest MSE achieved for each number of approximating vertices. From these results it is apparent that above a certain limit there is little to be gained by increasing the fineness of the approximation, while the computation time would be increased significantly. The cut-off point corresponds to the fineness that satisfies the thickness condition and therefore respects the object topology, assuming that the tolerance criterion is also satisfied.

7 EFFECT OF INITIAL MISALIGNMENT

Effect of the initial misalignment was investigated in order to determine how many iterations are on average required to achieve convergence. The three curves in Fig. 7 present typical results, which were obtained by fitting 200 measured points with random initial misalignments in the ranges of ± 15.0 mm/$\pm 15.0°$, ± 3.0 mm/$\pm 3.0°$ and ± 0.3 mm/$\pm 0.3°$. Each point on each curve represents an average result of 100 simulations. In all these cases the final accuracy of registration was the same and we conclude that initial misalignment affects only the speed of convergence.

Using the ICP method in these experiments, global convergence was achieved in all cases but one. In that one case the MoI method was successfully applied as the first alignment step, resulting in a better initial guess and subsequent global convergence.

8 EFFECTS OF THE MEASUREMENT NOISE AND THE NUMBER OF MEASURED POINTS

In this study it was important to conduct simulations such that the effects of different noise values and different numbers of measured points were analysed 'under the same circumstances', since there was only a finite set of simulation runs and a finite number of randomly generated measured points in each case. Thus in order to ensure *statistical reliability* (**10**) of the results, the same set of randomly generated initial positions was used in examining each combination of the measurement noise and the number of points.

The experiments were conducted using four different measurement noise values ($\sigma = 8\,\mu$m, $25\,\mu$m, $40\,\mu$m and $60\,\mu$m), eight different numbers of points (in the range of 20–10 000) and 100 different random initial positions. Thus a total of 3200 simulations were run. The results are shown in Figs 8 to 10.

With the different measurement noise and the different number of points in each experiment, the fitting error of the ICP method was analysed, this being the difference between the true transformation parameters (introduced as initial misalignment) and the estimated transformation. This difference also has its own probability distribution because of the randomness of the measurement noise and of the initial misalignment. It is common practice to summarize such a distribution in the form of *confidence limits*. In accordance with reference (**20**), the confidence statement for the case

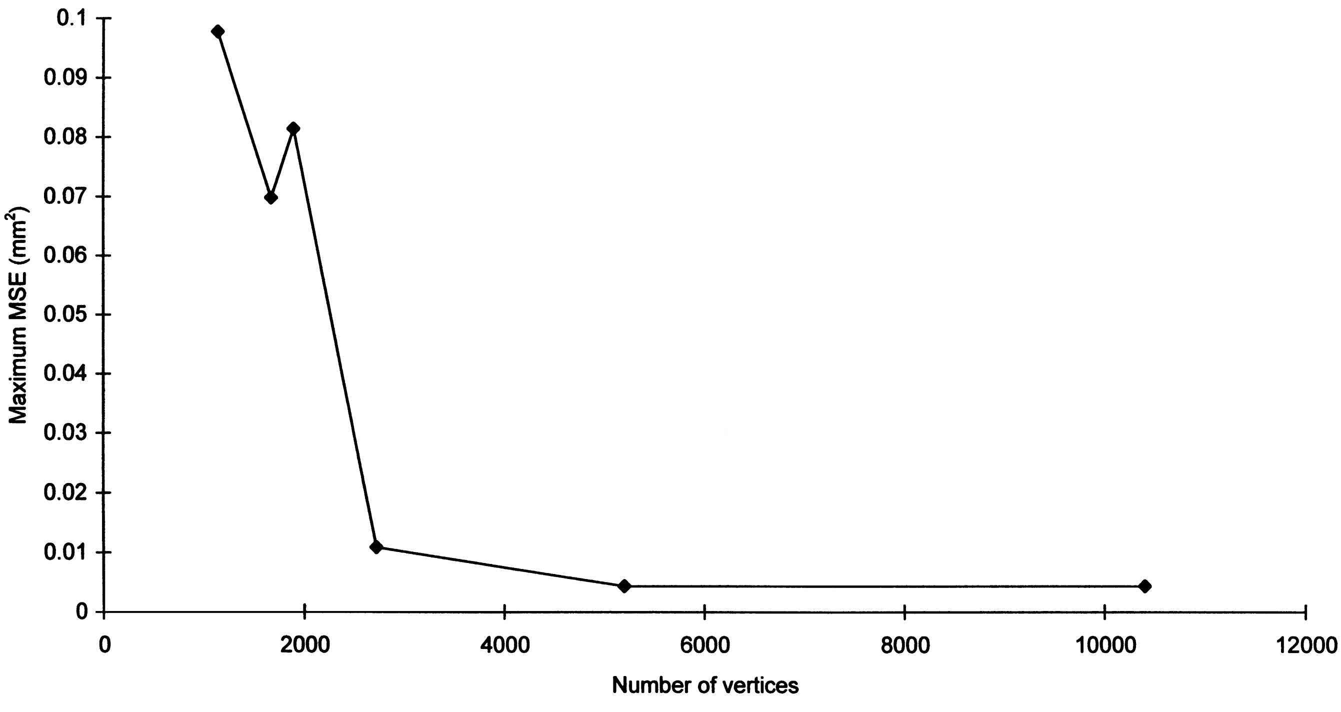

Fig. 6 Largest MSE after fitting versus number of vertices in approximation

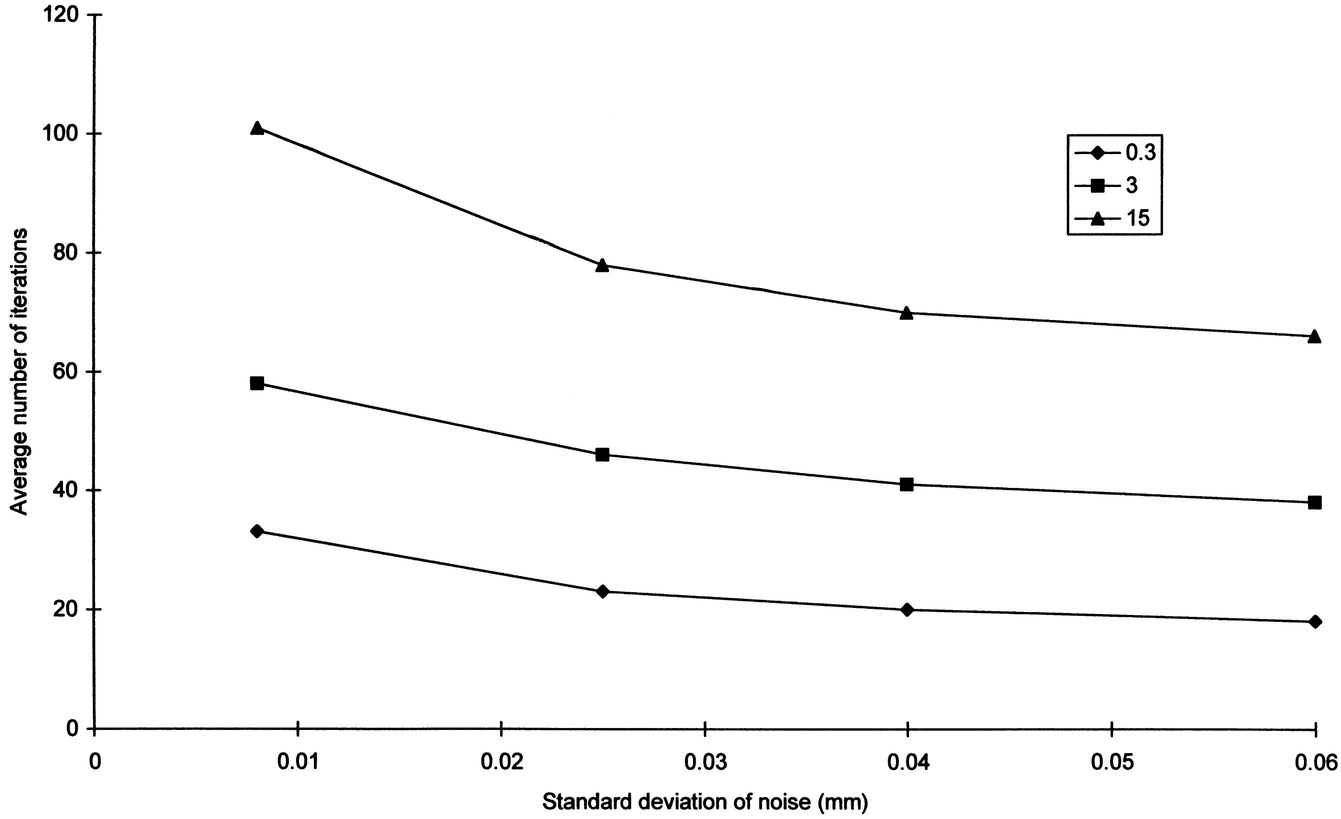

Fig. 7 Average number of iterations versus standard deviation of the measurement noise for different initial misalignments

of the mean value estimate μ of a random variable x is given by

$$\bar{x} - \frac{st_{\alpha/2}}{N} \leqslant \mu < \bar{x} + \frac{st_{\alpha/2}}{N}$$

where

$\bar{x} = \frac{1}{N}\sum_{i=1}^{N} x_i$ is the sample mean

$s^2 = \frac{1}{N-1}\sum_{i=1}^{N}(x_i - \bar{x})^2$ is the unbiased sample variance

$N =$ sample size

$t_{\alpha/2}$ is found from the Student t-statistic tables

For $N = 100$, as was the case in the present experiments, the difference between $t_{\alpha/2}$ and the normal critical value is very small. Nevertheless, the relevant metrology standards (such as DIN 1319) recommend that the confidence intervals be estimated using the above formulae and this recommendation was followed in this work.

Figure 8 presents examples of the confidence interval widths for rotation α and translation x, for different numbers of measured points and different noise values. Confidence, and therefore the accuracy of parameter estimates, clearly improves for a large number of points, but the size of the confidence interval can be seen to increase with larger noise. In fact, this should be expected, since perfect alignment would result in the error for each point being given by the measurement noise itself. Therefore, as explained in Section 5, the standard deviation of the noise sets the minimum achievable MSE in LS fitting.

The conclusion is that high registration accuracy requires both highly accurate measurements in order to minimize the achievable MSE and a large number of measured points such that this MSE value is achieved. This has important practical implications, especially when evaluating different sensors for a particular inspection application. For example, a touch-trigger probe offers high accuracy but its speed will generally make it feasible to collect only a small number of measurements. In contrast, a non-contact laser triangulation probe provides somewhat inferior accuracy, but it can rapidly collect a large number of measurements.

At the same time, however, the graphs in Figs 8 and 9 show that acceptable accuracy can be achieved with only 200–300 points. This is an important result which allows the conclusion to be made that in the initial stages of fitting, a smaller number of measured points may be used, thus improving the computational speed. When a minimum is reached, the full measurement set can then be continued. In the several hundred conducted experiments, this final stage required only one or two further iterations.

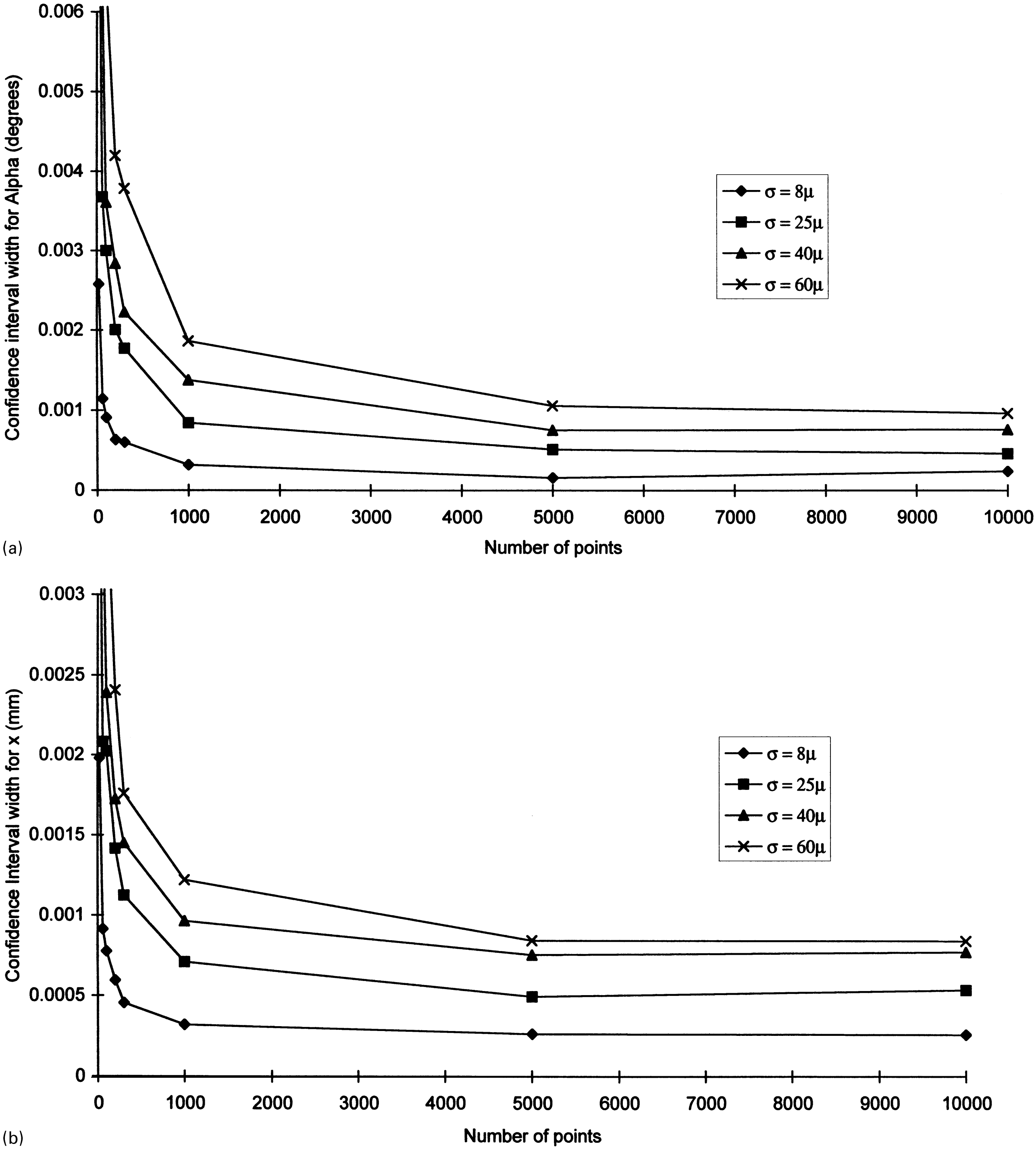

Fig. 8 Variation of the confidence interval width of parameter estimates versus number of measured points for different noise values. (a) Rotation α about the x axis; (b) translation along the x axis

9 EFFECTS OF GEOMETRY

The graphs in Figs 9a and b show the dependence of confidence in translation and rotation parameter estimates respectively, on the number of measured points (on a logarithmic scale), for a given noise value. They clearly show that the confidence is never equal for all parameters, which is a direct consequence of the object geometry. The position of the airfoil shape used in these experiments is relatively poorly defined with respect to the z axis position and rotation about the y axis (Fig. 1), and this is also evident from the confidence plots.

The graph in Fig. 10 further illustrates this situation. It shows that the mean error in transformation parameter

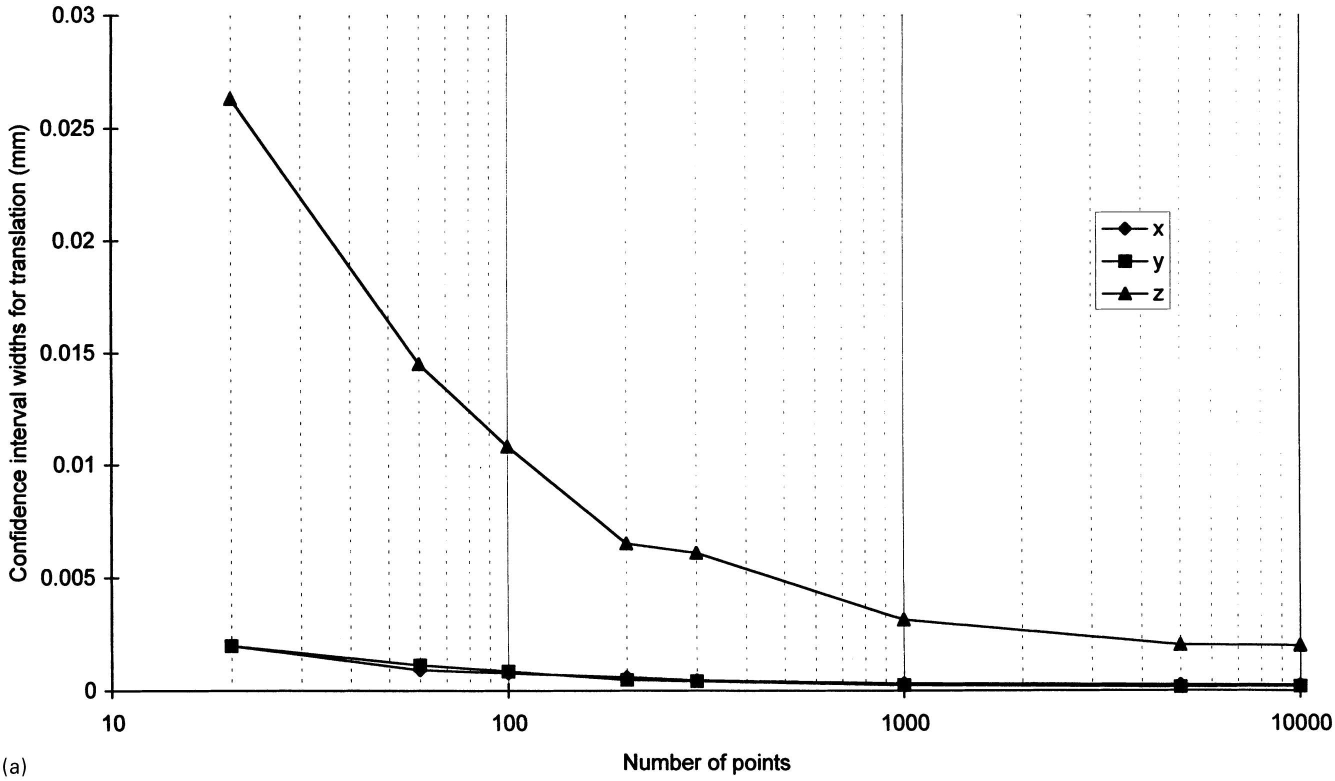

(a)

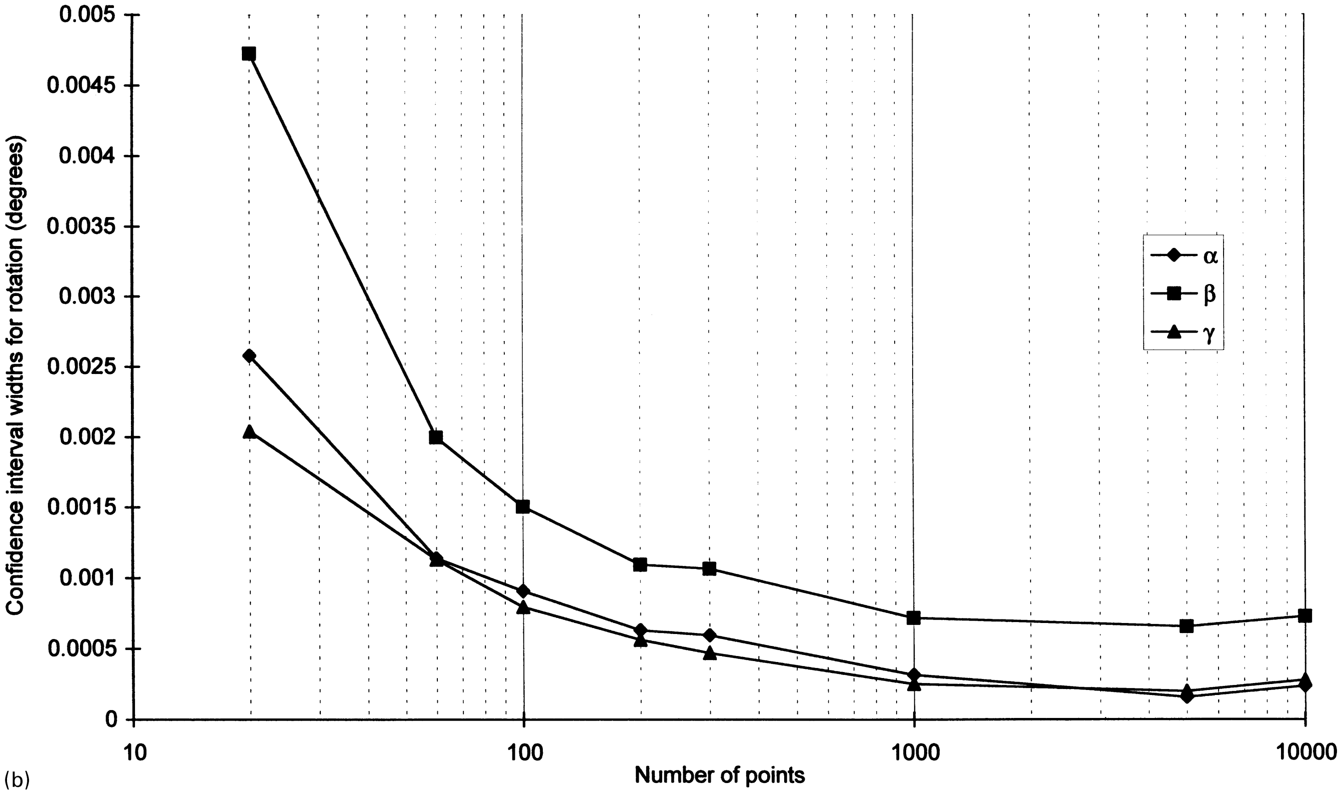

(b)

Fig. 9 Confidence interval width for parameter estimates versus number of measured points (noise $\sigma = 8\,\mu$m). (a) Translation parameters x, y, z; (b) rotation parameters α, β, γ

estimates tends to zero as the number of measured points increases, as expected on the basis of the global convergence of the ICP algorithm. However, the difference between the curves clearly indicates that it is the poor determinacy of the position in the *z* direction that demands the use of a larger number of points.

These results show that for a given complex geometry there are no easy answers about how many measurements are required to achieve registration to a given accuracy. The conclusion drawn from this work is that the optimal solution to the problem should be sought through extensive simulation of the measurements for the given object, from which the acceptable lower limit for the point density can be derived.

10 CONCLUSIONS

This paper is concerned with accurate registration as demanded by the purposes of dimensional inspection of free-form surfaces. Registration of surfaces defined as NURBS was implemented using the ICP method, as a realization of LS fitting. The influence of a number of important factors was analysed, one of the most important ones for inspection purposes being the measurement noise.

Quality of fit was measured using confidence in the transformation parameter estimates. The results clearly show that in the presence of measurement noise, as is always the case in practice, confidence improves with an increased number of measured points. This is an important result for inspection, which confirms the intuitive reasoning that measuring a very large number of points with lower accuracy can provide better results than measuring a very small number of points with higher accuracy. This has important implications when evaluating different measurement technologies for a given application.

At the same time it was concluded that precision of registration does depend on the precision of measurement. This is because the MSE after fitting was found to approach the MSE of the measurements and because the confidence interval for transformation parameter estimates becomes narrower for lower noise.

The amount of initial misalignment was found to affect the number of required ICP iterations, as would be expected. However, the highly encouraging result was that global convergence of ICP was achieved in almost all of the *several thousand* experiments, while the problems encountered in a few cases with large initial misalignment were readily overcome by applying the MoI method as the first alignment step.

One of the most important factors affecting registration performance was confirmed to be the shape of the object,

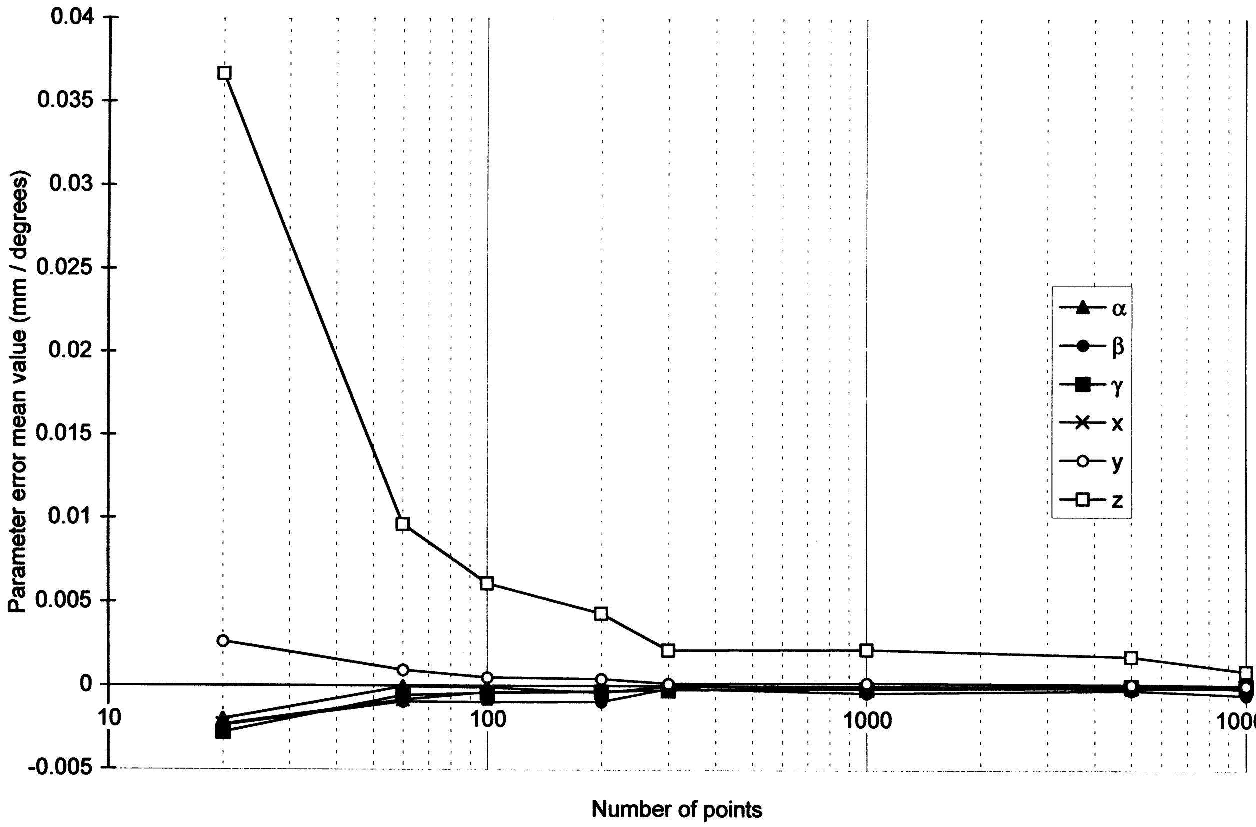

Fig. 10 Mean error in transformation parameter estimation versus number of measured points (noise $\sigma = 8\ \mu m$)

in particular the degree of symmetry about any axes and the definition of the object position by the measured points. Ill-conditioning of a given geometry in terms of LS fitting is reflected in the slower convergence rate with respect to the particular degrees of freedom. For the object used in this study it was the translation along the z axis that was most pronounced in this respect, followed by rotation α about the x axis. However, in all of the conducted experiments it was still possible to achieve global convergence to within the prescribed tolerance.

Iteration termination criteria have been found to be the key for achieving high registration accuracy. The criterion based on the known noise variance, σ, as presented, was found to produce the required results.

The investigation has also confirmed that accurate registration requires a large number of iteration steps. This was the main incentive for maximizing the computational efficiency of each iteration and the adoption of dual representation of the NURBS model has significantly improved the overall computing time. Importantly, the results have also shown that beyond a certain point, increased fineness of approximation brings diminishing benefits, while the computation time increases linearly with the number of approximating points. The cut-off point was found to correspond to the fineness that adheres to the object thickness criterion, which must be satisfied.

Finally, in the absence of readily available analytical techniques, Monte Carlo simulation was shown to be a good tool for assessing the registration performance in a given situation. The simulation process described in the paper can be readily performed, in full or in part, to produce definitive results about registration of any given object using any given measurement sensor.

REFERENCES

1 **Jain, R.** and **Jain, A.** Report on Range Image Understanding Workshop, held in East Lansing, Michigan, 21–23 March 1988. *Machine Vision and Applications*, No. 2, 1989, pp. 45–60 (Springer-Verlag, New York).

2 **Newman, T. S.** and **Jain, A. K.** A survey of automated visual inspection. *Comp. Vision Image Understanding*, March 1995, **61**(2), 231–262.

3 **Besl, P. J.** *Surfaces in Range Image Understanding*, 1988 (Springer-Verlag, New York).

4 **Besl, P. J.** and **McKay, N. D.** A method for registration of 3-d shapes. *IEEE Trans. Patt. Ann. Mach. Intell.*, February 1992, **14**(2), 239–255.

5 **Menq, C. H., Yau, H. T.** and **Lai, G. Y.** Automated precision measurement of surface profile in CAD-directed inspection. *IEEE Trans. Robotics Automn*, April 1992, **8**(2), 268–278.

6 **Haralick, R. M., Joo, H., Lee, C., Zhuang, X., Vaidya, V. G.** and **Kim, M. B.** Pose estimation from corresponding point data. *Machine Vision for Inspection and Measurement*, 1989 (H. Freeman, New York Academic).

7 **Pennec, X.** and **Thirion, J.-P.** Validation of 3-D registration methods based on points and frames. In Fifth International Conference on *Computer Vision*, Cambridge, Massachusetts, 1995, pp. 557–562 (IEEE, Piscataway, New Jersey).

8 **Eggert, D. W., Lorusso, A.** and **Fisher, R. B.** Estimating 3-D rigid body transformations: a comparison of four major algorithms. *Mach. Vision and Applic.*, 1997, **9**(5/6), 272–290.

9 **Stoddart, A. J., Lemke, S., Hilton, A.** and **Renn, T.** Estimating pose uncertainty for surface registration. In British Machine Vision Conference, Edinburgh, Scotland, 1996.

10 **Shreider, Y. A.** *Method of Statistical Testing–Monte Carlo Method*, 1994 (Elsevier, Oxford).

11 **Lin, Z. C., Lee, H.** and **Huang, T. S.** Finding 3-D point correspondences in motion estimation. In Eighth International Conference on *Pattern Recognition*, 1986, pp. 303–305 (IEEE, New York).

12 **Arun, A., Huang, T. S.** and **Blostein, S. D.** Least square fitting of two 3-D point sets. *IEEE Trans. Patt. Analysis Mach. Intell.*, 1987, **PAMI-9**(5), 698–700.

13 **Ristic, M.** and **Brujic, D.** Efficient registration of NURBS geometry. *Image Vision Comp.*, 1997 (in press).

14 **Brujic, D.** and **Ristic, M.** Analysis of free-form surface registration. In Proceedings of IEEE International Conference on *Image Processing*, Lausanne, Switzerland, 16–19 September 1996, Vol. 2, pp. 393–396 (IEEE, Piscataway, New Jersey).

15 **Von Herzen, B.** and **Barr, R. M.** Accurate triangulations of deformed, intersecting surfaces. *Comp. Graphics*, July 1987, **21**(4), 103–110.

16 **Lane, J. M.** and **Carpenter, L. C.** A generalised scan line algorithm for the computer display of parametrically defined surfaces. *Comp. Graphics Image Processing*, November 1979, **11**(3), 290–297.

17 **Faugeras, O.** *Three-Deminsional Computer Vision: A Geometric Viewpoint*, 1993 (MIT Press, Cambridge, Massachusetts).

18 **Kanatani, K.** Analysis of 3-D rotation fitting. *IEEE Trans. Patt. Analysis Mach. Intell.*, 1994, **16**(5), 543–549.

19 **Dietrich, C. F.** *Uncertainty, Calibration and Probability*, 1991 (Adam Higler, Bristol).

20 **Bendat, J. S.** and **Piersol, A. G.** *Measurement and Analysis of Random Data*, 1996 (John Wiley, New York).